LBL-25119

Lawrence Berkeley Laboratory
UNIVERSITY OF CALIFORNIA

Engineering Division

Presented at the IEEE 1988 Nuclear Science Symposium,
Orlando, FL, November 9–11, 1988, and to be published
in IEEE Transactions on Nuclear Science

Optical Receivers for Wide Band Data Transmission Systems

B. Leskovar

April 1988

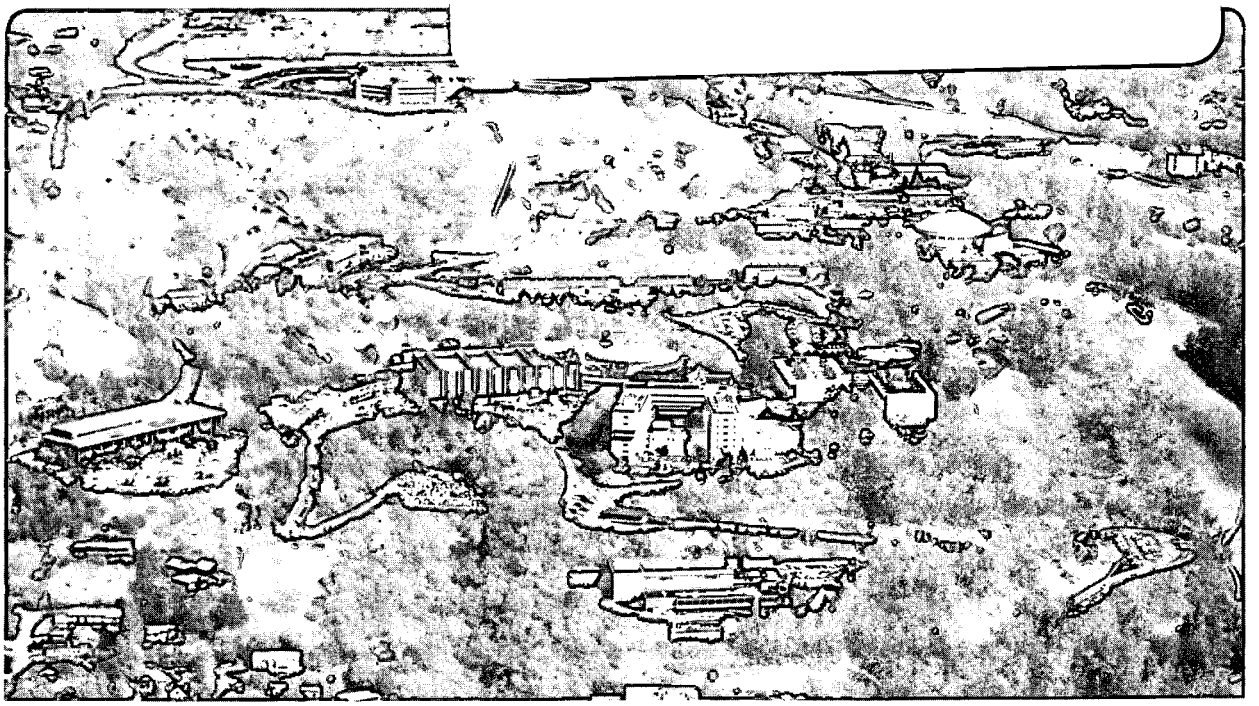

Prepared for the U.S. Department of Energy under Contract Number DE-AC03-76SF00098.

DISCLAIMER

LBL-25119

Optical Receivers for Wide Band Data Transmission Systems

Branko Leskovar

Engineering Division
Lawrence Berkeley Laboratory
1 Cyclotron Road
Berkeley, California 94720

April 1988

OPTICAL RECEIVERS FOR WIDE BAND DATA TRANSMISSION SYSTEMS

Branko Leskovar
Lawrence Berkeley Laboratory
University of California
Berkeley, California 94720 U.S.A.

ABSTRACT

Optical receiver designs for digital fiber data transmission systems operating with Gbit/s data rates in the 800 - 1500 nm wavelength region have been investigated. The tradeoffs between conflicting receiver design requirements are considered in detail. The state-of-the-art performance of photodetectors and low-noise amplifiers is discussed. Also, present receiver performance data, such as sensitivity, dynamic range, bit rate and bit pattern dependencies as a function of the bit rate in the 0.01 - 8 Gbit/s data rate range are summarized and reviewed.

INTRODUCTION

The concept of guided lightwave communication along optical fibers has stimulated a major new technology over the past two decades. Fiber optic links provide a number of major advantages over conventional electronic communication systems, such as immunity to electromagnetic interference, and low transmission losses at very high data rates. It also makes possible thinner and lighter cables and has a strong potential for tens-of-kilometer-long repeaterless link capabilities extending into the gigahertz region.

The emergence of optical communication using fibers was made possible by the parallel development of low loss fibers, heterojunction lasers, light-emitting diodes (which emit in spectral regions of low fiber loss) and sensitive photodetectors. The technology of optical fiber communication systems is advancing at a very rapid rate. Significant advances have been made in the fabrication of low-loss and low dispersion optical fibers. Losses of only 0.27 dB/km at 1300 nm wavelength have been achieved for single mode fibers. Furthermore, the development of optical sources and optical receivers, for long wavelength applications is also advancing rapidly. Several experimental transmission systems capable of operating at a 8 Gbit/s rate over a distance of 30 km and 4 Gbit/s rate over a distance of 117 km have been reported.[1-2] Although these results were obtained under highly optimized operating conditions they do give an indication of future capabilities. At present practical high data rate optical transmission systems are operating between 90 Mbit/s and 565 Mbit/s.

The local data communication needs have given a new impetus for the development of advanced system components. The recent systems for local communication, such as computer interconnections and instrumentation for basic and applied research, have made necessary a high data rate capability. Specifically, instrumentation systems, using wide amplitude dynamic range and high spatial resolution charge-coupled device image sensors[3-5] require an extraordinarily high data rate transfer capability. For example in the Superconducting Super Collider detector and accelerator systems, high capacity fast fiber links will have a widespread application.[6-7]

The optical fiber receiver design requires careful attention for data transmission systems having a high-bit-rate capability. The receiver performance characteristics, such as sensitivity, dynamic range, bit rate transparency, bit pattern independency and acquisition time are functions of both the photodetector and receiver preamplifier configuration as well as operating bit rate. The receiver design for fiber data transmission has been addressed in various papers.[8-13] Most of these papers have dealt with receivers for telecommunication applications. Although the tradeoffs between conflicting receiver design requirements, for operation in the 0.01-8 Gbit/s data rate range, are limited in our considerations to digital systems, the results obtained can be easily modified and applied to optical receiver design for analog transmission and sensing applications.

RECEIVER CHARACTERISTICS AND DESIGN CONSIDERATIONS

A simplified block diagram of a typical digital optical receiver is shown in Fig. 1. The input optical signal is detected by a photodetector. The photodetector is followed by a low-noise preamplifier, an automatic gain control amplifier and a shaping filter. The regenerator samples the detected signal and regenerates the original data that is being transmitted. The shaping filter minimizes of noise and intersymbol interference at the regenerator input. The clock pulses required for sampling are recovered by the timing extraction circuitry which is typically phase-locked-loop. The most important components in determining receiver performance are the photodetector and low-noise preamplifier.

Photodetector Characteristics

The most useful photodetectors for optical fiber systems are the PIN and avalanche photodiode. The APD is more sensitive than the PIN diode because of its internal avalanche gain. For the wavelength region around 850 nm photodiodes are fabricated from germanium and several III-V compounds (InGaAsP, GaAlAsSb). At present long-wavelength transmission systems have achieved better performance with III-V compounds APD's than with Ge APD's. Ge APD's have relatively higher dark current, unfavorable ratio of ionization coefficients and low absorption coefficient compared with III-V compounds APD's at these wavelengths. The APD structure which has achieved very good performance to date has separate absorption and multiplication regions (SAM-APD's).

The ADP's of this type utilize InP in the multiplication region and a lattice-matched epitaxial layer of InGaAs in the absorbing region. The SAM APD's were developed to eliminate the tunneling component of the dark current in InGaAs APD's. In this structure the p-n junction, and thus the high field region, is located in InP where tunneling is insignificant and absorption occurs in an adjacent layer of InGaAs. To improve the frequency response of the SAM APD's single (or more) InGaAsP transition layer(s) is interposed between the InP multiplication region and the InGaAs absorption region. The transition layer(s) grade stepwise bandgap energy between that of InP and InGaAs. The net effect of adding the transition layer(s), is to reduce the valence band discontinuity which results in an elimination of most of the charge accumulation at the heterojunction interface. Such structure is called SAGM-APD, where G denotes the presence of one or more grading layers.

Because conventional PIN photodiodes and APD's for fiber data transmission have been discussed elsewhere[13-16] only SAGM-APD's will be discussed here in detail. A schematic cross section of the InP/InGaAsP/InGaAs SAGM-APD with a single grading level is shown in Fig. 2. The thin grading layer of InGaAsP was Sn-doped. The top layer, an n^- InGaAs absorbing region was grown thick ($\cong 7\mu m$) in order to keep the edge of the depletion region away from the n^- type contact. Following crystal growth, mesa diode was fabricated by etching. A window is open in the substrate metallization to permit back

illumination. Chip was mounted in a low-capacitance (<0.1 pF) pill package. Light is essentially absorbed in the depleted portion of the InGaAs layer.

The frequency dependance of the avalanche gain of the SAGM-APD, which is determined by the RC time constant, the transit time of carrier through the space-charge region and residual charge accumulation at the heterojunction interfaces, is approximately given by the following expression[11-13]:

$$\frac{M(\omega)}{M_0} \cong T(\omega)\left\{\left[1+\left(\frac{\omega}{e_h}\right)^2\right][1+(\omega RC)^2][1+(\omega\tau_e M_0)^2]\right\}^{-1/2} \quad (1)$$

where M_0 is dc avalanche gain, ω is the radiant frequency, $T(\omega)$ is normalized transit time factor, e_h is the emission rate for holes trapped at the heterojunction interface, R is the sum of APD series resistance and load resistance, C is the diode capacitance and τ_e is the effective transit time through the multiplication region.

The transit time factor $T(\omega)$ in equation (1) accounts for the time required for the primary and secondary carriers to drift across the depletion region. Transit time is not a limiting factor for the device frequency response for frequencies less than 10 GHz with total depletion width of 3 μm.

The RC time constant of a packaged SAGM-APD is typically in the range of 6-20 ps. The minimum and maximum bandwidths associated with this parameter is 8 and 26 GHz.

The hole emission rate, $1/e_h$, is typically smaller than 15 ps for devices having single grading level. It is smaller than 5 ps for devices with multiple transition layers. Consequently, bandwidths of 2 GHz and 5,5 GHz have been achieved with SAGM-APD's at dc avalanche gain of M_0 = 9 using single transition layer and three intermediate-bandgap layers, respectively.

The term $\omega\tau_e M_0$ in equation (1) originates from the device avalanche buildup time. In general, the higher the avalanche gain the longer it takes the avalanche process to build up. The avalanche build up time and hence the device gain-bandwidth product is essentially determined by the ratio of the electron and hole ionization coefficients. It was shown previously[11] that a higher bandwidth can be achieved the more these coefficients differ for a given dc avalanche gain M_0. For the SAGM-APD the coefficient values are determined by the bulk crystal properties of the multiplication region. However, structural modifications, such as use of a low-high doping profile in the multiplication region and a reduction of the region width, can provide an improvement in the gain-bandwidth product. Recently, it has been shown[15] that in an experimental back-illuminated mesa structure the gain-bandwidth product was increased from 18 to 70 GHz by reducing the multiplication layer thickness from 1.5 μm to less than 0.5 μm. Consequently, by optimizing appropriately the device parameters, SAGM-APD's can achieve the high bandwidths required for multigigabit optical receivers.

The state-of-the art performance of three representative photodetectors for long wavelengths (1000 - 1600 nm) optical fiber data transmission systems are summarized in Table I. They include InGaAs APD, InGaAs PIN and InP/InGaAsP/InGaAs SAGM-APD. Also characteristics of a Si APD for 800-900 nm wavelength region are presented for comparison. It can be seen that the optical performance is comparable for InGaAs APD and PIN photodetectors. They have a quantum efficiency of approximately 80%, response time of 100 ps and a diode capacitance smaller than 1 pF. The SAGM-APD device with optimized parameters exhibits excellent performance, such as dark current of 2-50 nA, ionization ratio of 0.35, and avalanche gain-bandwidth product of 70 GHz.

Digital Receiver Sensitivity

In analyzing the sensitivity of optical digital receivers employing PIN or avalanche photodetectors the noise spectrum is assumed to be Gaussian.

As receiver bandwidth is increased to accommodate higher transmission bit rates its sensitivity decreases mostly because the preamplifier noise increases rapidly with bit rate. The receiver sensitivity is defined as the minimum optical power level required at the receiver input so that it will operate reliably with a bit error rate less than a desired value. In this case it is given as the average optical power $\bar{P}$ required for a bit error rate, (BER), of 10^{-9}.

Bit error rate is defined as the ratio of bits incorrectly identified to the total number of bits transmitted. The receiver sensitivity is also often specified in terms of the average optical power $\eta\bar{P}$ which is detected by the photodetector, where η is the quantum efficiency of the photodetector. Until recently, PIN photodiodes fabricated from InGaAsP alloys grown epitaxially on high quality InP substrates were regarded, as most suitable for use in the low-noise optical receivers of long wavelength communication systems. However, recently, at high bit rates, reverse biased, avalanche photodiodes exhibit high-speed response in the absence of large dark currents. In this section the source of noise in receivers employing PIN and avalanche photodetectors will be discussed and their sensitivities compared.

Depending on their configuration, preamplifiers for optical receiver are classified into two types: high impedance and transimpedance designs, Fig. 3. The high impedance preamplifiers offer the lowest noise level and hence the highest detection sensitivity. However, the frequency response is limited by the RC time constant at the input making necessary an equalizer following the preamplifier to extend the receiver bandwidth. Furthermore, this design has a limited dynamic range due to the high-input load resistance. The transimpedance amplifiers have a large dynamic range and bandwidth due to their negative feedback. However, because of the thermal noise of the feedback resistor the preamplifier noise level is higher and sensitivity is lower than that of a high-impedance design.

The following sections discuss the noise characteristics of preamplifiers using bipolar junction transistor and FET and the sensitivity that can be achieved with PIN and ADP detectors.

The receiver sensitivity in terms of average detected optical power $\bar{P}$ required at the receiver input for a desired bit error rate with a PIN photodiode used as the signal source, is given by

$$\eta\bar{P} = Q\frac{hc}{e\lambda}(\langle i_n^2\rangle)^{1/2} \quad (2)$$

where η is the quantum efficiency of photodiode, h is the Planck's constant, c is the velocity of light, e is the electron charge, λ is the wavelength and Q is a parameter determining error rate in digital systems. The term $\langle i_n\rangle$ represents the input equivalent rms noise current of the preamplifier. The parameter Q relates to the desired bit error rate BER by the following expression:

$$BER = \frac{1}{(2\pi)^{1/2}}\int_Q^\infty \exp\left(-\frac{x^2}{2}\right)dx \quad (3)$$

$$Q = \frac{D - S_{0,1}}{\sigma_{0,1}} \quad (4)$$

Here $S_1(S_0)$ is the expected value of signal associated with a mark (space), σ_1 (σ_0) is its variance and D is the decision level set by the optical receiver. The bit error rate as a function of Q is shown in Fig. 5. It is seen from this figure that for a BER = 10^{-9} the value of parameter Q = 6.

For microwave bipolar junction transistor preamplifier the principal noise sources are shot noise from the base-spreading resistance r_{bb} and thermal noise from the load or feedback resistor. At the optimum bias current the rms input noise current is approximately given by[8-10]

$$\langle i_n^2 \rangle \cong \frac{4kT}{R_f} A_2 B + 8\pi kT C_0 \left(\frac{A_2 A_3}{\beta} \right)^{1/2} B^2 + \\ + 4(2\pi)^2 A_3 [e\alpha C_0 V_T^{\,2} + kT r_{bb} C_{dsf}^2] B^3 \qquad (5)$$

where B is the operating bit rate, k is the Boltzmann's constant, T is the absolute temperature, R_f is the feedback resistance in transimpedance design or load resistance in high impedance design, A_2 and A_3 are the weighting functions[8] which are dependent only on the input optical pulse shape to the receiver and the equalized output pulse shape. For the rectangular non-return-to-zero (NRZ) coding format and equalized output pulse with a full raised cosine spectrum A_2 = 0.562 and A_3 = 0.0868. For the return-to-zero (RZ) coding format with 50% duty cycle A_2 = 0.403 and A_3 = 0.0361. Other terms in equation (5) are: β is the transistor current gain, e is the electron charge, $\alpha = \tau_F / V_T$ (τ is the forward transit time, V_T = kT/e), C_0 is the total input capacitance under zero bias current conditions, $C_{dsf} = C_{ds} + C_f$ (C_{ds} is the photodetector and stray capacitance, C_f is the feedback capacitance). Microwave silicon bipolar transistors typically have α = 0.6 - 0.8 pF/mA and β = 100.

For the high-impedance preamplifier design the first noise term, that is due to the load resistance, can be neglected. Thus, the input equivalent noise power varies as the square of the operating bit rate until at very high rates the last term involving B^3 become dominant. In this case the noise power varies with bit rate between B^2 and B^3.

For transimpedance preamplifier design, the feedback resistor should be reduced as the operating bit rate increases in order to accommodate the wider bandwidth requirement. In general, the reduction in feedback resistance R_f is in inverse proportion to the bit rate increase. In this case the input noise power varies as the square of the bit rate until B^3 dependence becomes dominant. For FET preamplifier the principal noise sources are Johnson noise associated with the FET channel conductance, Johnson noise from the load or feedback resistor, shot noise arising from gate leakage current and 1/f noise. The rms input noise current is approximately given by[8-10]

$$\langle i_n^2 \rangle \cong \left(\frac{4kT}{R_f} + 2eI_L \right) A_2 B + \frac{4kT\Gamma}{g_m} (2\pi C_T)^2 A_f f_c B^2 + \\ + \frac{4kT\Gamma}{g_m} (2\pi C_T)^2 A_3 B^3 \qquad (6)$$

where B is the operating bit rate, A_f is the weighting function (for NRZ coding format A_f = 0.184 while for RZ coding format with 50% duty cycle A_f = 0.0984), I_L is the total leakage current (FET gate current and dark current of photodiode), g_m is the FET transconductance, Γ is a noise factor associated with channel thermal noise and gate induced noise in the FET (Γ = 0.7 -1.0 for Si FET's and Γ = 1.1 -1.8 for GaAs MESFET), C_T is the total input capacitance consisting of photodiode and stray capacitance and f_c is the 1/f corner frequency of the FET. Definition of other terms is the same as for equation (5).

A close inspection of expression (6) shows that the noise can be minimized by making the feedback or load resistance R_f as large as possible. However, there is tradeoff between the receiver sensitivity and dynamic range in the choice of R_f, since the maximum signal level which can be processed by the receiver without saturation decreases as R_f becomes larger. Consequently, the receiver can be designed with lower than optimum values of R_f from the noise standpoint in order to provide wider dynamic range.

It can be also seen from (6) that the total leakage current I, consisting of FET gate current and the photodiode dark current should be as small as possible. It is also desirable to choose an FET with low gate leakage current, low input capacitance, high transconductance and low 1/f noise corner frequency. For a high-impedance FET preamplifier design the noise power at high bit rates is dominated by the thermal channel noise. In this case the noise power varies with the third power of the bit rate. Furthermore, noise power is proportional to the total input capacitance. Consequently, a decrease of this capacitance by hybrid or integrated circuit fabrication significantly improves low-noise performance.

The receiver sensitivity in terms of average detected optical power P required at the receiver input for a desired bit error rate where an avalanche photodiode is used as the signal source is approximately given by

$$\eta \bar{P} \cong Q \frac{hc}{e\lambda} \left[QeF(M) A_2 B + \left(\frac{\langle i_n^2 \rangle}{M^2} + 2eI_{dm} F(M) A_2 B \right)^{1/2} \right] \qquad (7)$$

where B is the operating bit rate, F(M) is the avalanche excess noise factor defined by

$$F(M) = kM + (1-k)(2 - 1/M) \qquad (8)$$

where k is the ratio of the ionization constant of holes and electrons in the photodiode ($k \leq 1$), and M is the avalanche gain. The term I_{dm} in equation (7) is the primary component of the APD dark current which undergoes multiplication process.

Other terms in equation (7) are the same as previously defined for the expressions (5) and (6).

From above given expressions the equivalent input noise power can be calculated as a function of the operating bit rate. The calculated values assuming the NRZ coding format are shown in Fig. 6 for the following three preamplifier designs: microwave Si bipolar junction transistor transimpedance and high impedance preamplifier, and GaAs FET high impedance preamplifier. FET transimpedance design is not presented because its performance is essentially the same as the transimpedance Si bipolar transistor preamplifier design. The typical transistor parameter used for these calculations were: C_{ds} = 0.5 pF, I_{dn} = 1 nA, $I_{dm} = I_{nA}$ (for InGaAs APD), I_{dm} = 1 pA (for Si APD), k = 0.3 (for InGaAs APD), k = 0.03 (for Si APD), β = 100, C_0 = 1.5 pF, α = 0.6 pF/mA, r_{bb} = 20Ω, g_m = 15 mS, C_{gs} = 0.2 pF, I_g = 1 nA, f_c = 30 MHz, C_{dsf} = 0.5 pF, R_f X B = 750 kΩX Mbit/s (for transimpedance amplifier), and I_L = 2 nA.

It can be seen from Fig. 6 that the FET high impedance preamplifier provides the lowest noise level. In general, the advantage of the FET high impedance design over the bipolar transistor high impedance and transimpedance designs is reduced as the operating bit rate increases. As a matter of fact the FET noise power increases at a faster rate than the bipolar transistor noise power with an increase of the operating bit rate. Thus above 5 Gbit/s the bipolar transistor application can result in a smaller noise power level. The exact crossover point is dependent on particular characteristics of the photodiode and receiver preamplifier components.

Also included in Fig. 6 are calculated values of the optical receiver sensitivity for three preamplifier designs using InGaAs

avalanche photodiode considered previously and PIN photodiode-FET preamplifier. It can be seen from the figure that if PIN photodiode is used, a low-noise FET preamplifier is necessary to achieve high sensitivity. Furthermore, it can be seen that InGaAs APD's offer receiver sensitivity which is approximately 5-10 db better than PIN FET receivers at high operating bit rates.

Germanium avalanche photodiodes can be also used in receiver designs. The sensitivity of a Ge APD receiver is more dependent on temperature because of dominant noise effect of their dark current. Furthermore, Ge APD receiver sensitivity is for 5-10 dB lower than that of a receiver of the same design using InGaAs APD.

The dependence of the receiver sensitivity on the preamplifier noise current can be determined from expressions (5), (6) and (7). For PIN photodiodes the receiver sensitivity is proportional to $<i_n>^{1/2}$. For InGaAs APD with value of k $\cong$0.3 and negligible dark current the receiver sensitivity is approximately proportional to $<i_n>^{1/4}$. Also from the same expressions the optimum avalanche gain can be calculated as a function of bit rate for various photodetector and preamplifier designs. In general, the optimum avalanche gain is such that the photodetector shot noise is comparable to receiver preamplifier noise. Thus the optimum avalanche gain is higher for a photodetector having lower dark current and lower excess noise. Similarly, optimum gain is lower for a preamplifier having lower noise level. Typically, the optimum avalanche gain values are from 10 to 35 for InGaAs APD. For the SAGM APD's, having k = 0.35, the optimum gain is approximately 12 at a bit rate of 5 Gbit/s.

At very high bit rates, the limiting gain-bandwidth product, f_{GB}, of an avalanche photodiode can prevent operation at the optimum gain causing a decrease of the receiver sensitivity. Using equation (7) calculations have been made for a 1300 nm APD with k = 0.35 and f_{GB} values of 20 and 50 GHz assuming negligible intersymbol interference and preamplifier with GaAs FET having f_T = 20 GHz, C_d = 0.5 pF and I_{GATE} = 100 nA. Calculations have shown that at 5 Gbit/s data rate the sensitivity decrease is 1 and 4 dB for photodiode with f_{GB} = 50 GHz and 20 GHz, respectively.

The dark current of a photodetector degrades the receiver sensitivity, as shown in Fig. 5, depending upon the operating bit rate. Our studies have shown that for a PIN FET preamplifier, having a photodetector dark current of 10 nA, the receiver sensitivity will be reduced by 0.5 and 0.1 dB from values given in Fig. 5 for bit rates of 10 Mbit/s and 100 Mbit/s, respectively. For an InGaAs ADP's with k = 0.3 and dark current of 6 nA the receiver sensitivity will be reduced by 0.5 dB at 1 Gbit/s.

Similarly, the optical receiver sensitivity is reduced from characteristics shown in Fig. 5 if receiver operates over a wide range of bit rates. This is caused by the bit rate dependancy of the receiver preamplifier, the shaping filter and the timing recovery circuitry. In general, the design of these components is optimized at a given bit rate for the best receiver performance. Detailed studies have shown that typically for two to one data rate dynamic range, the receiver sensitivity is decreased from 3 to 4.5 dB and from 1.5 to 2.2 dB for PIN photodiode and InGaAs APD receiver, respectively. Therefore to accommodate widely different bit rates some component changes are necessary to keep the highest receiver sensitivity. Similar considerations for decrease of the receiver sensitivity can be applied in a case when receiver operates with different digital data coding formats.

Receiver Dynamic Range Considerations

As the received optical power level increases from the minimum detectable value (receiver sensitivity) the receiver bit error rate decreases because of higher signal-to-noise ratio of the preamplifier input signal. Improved performance continues until overloading occurs at the preamplifier. At this point the received signal waveform becomes distorted and the bit error rate starts to increase due to intersymbol interference. The maximum allowable optical power at the receiver input is defined as a level where the bit error rate becomes larger than the desired value. (In our case larger than BER = 10^{-9}).

The dynamic range is a function of the load resistor, or the feedback resistor, of the receiver preamplifier (depending upon the preamplifier design). As the load or feedback resistor decreases the maximum allowable received optical power increases, thus increasing the dynamic range. However, a reduction in load or feedback resistance results in an increase of the amplifier noise level, (equations 5 and 6). Consequently, there is a trade-off between the high receiver sensitivity and wide dynamic range. The typical dynamic range of a high impedance FET preamplifier and a transimpedance bipolar transistor design is shown in Fig. 6. It can be seen that a high impedance PIN FET preamplifier has typically an optical dynamic range of 15-20 dB. If an APD is used the dynamic range can be increased from 5 to 15 dB by incorporating the avalanche gain in the AGC feedback loop. Furthermore, it can be seen from Fig. 6 that the receiver dynamic range can be increased to 30-40 dB range when a transimpedance preamplifier design is used. However, it can be seen in this case from Fig. 5 that the receiver sensitivity will be decreased.

CONCLUSIONS

Very high speed avalanche photodiodes and high-sensitivity optical receivers will have considerable impact on future Gbit/s data transmission systems. Results of experimental receiver sensitivities as reported in literature for bit rates up to 8 Gbit/s are summarized in Table 2. In general, the receiver sensitivities are still approximately 20 dB above the quantum limit due to the lack of low noise long-wavelength APD's and imperfections of the receiver electronic circuitry. The highest experimental sensitivities have been obtained with InGaAs APD's and high impedance GaAs FET preamplifiers. These best results are still lower than theoretical sensitivities, calculated from equations (5), (6) and (7) for an APD receivers with ionization ratios of k = 0.35, by 3dB at 1 Gbit/s and 8 dB at 8 Gbit/s. The larger difference at the higher bit rate reflects both the limited APD gain-bandwidth product and greater difficulties achieving ideal operation of the electronic circuitry at very high bit rates. Electronic components and subassemblies for bit rates near 1 Gbit/s, such as preamplifiers, decision circuits, multiplexers, and demultiplexers have very good performance. However the same components at 4 and 8 Gbit/s are still in the experimental stage and they will require considerable development before the performance obtained at lower data rates. Limited capabilities of 8 Gbit/s electronics components and circuitry causes inter-symbol interference and imperfect receiver equalization.

The 420 Mbit/s and 1 Gbit/s receivers have demonstrated sensitivity of -46.2 dBm and -42.1 dB, respectively.[11] These receivers employed APD with 18 GHz gain-bandwidth product, dark currents I_{dm} = 2 nA and quantum efficiencies η = 95%. The receivers used high value of load resistors in order to maximize the sensitivity. Results obtained are within 4-6 dB of the best results obtained for the receiver sensitivity employing Si APD's.

The measured sensitivity of the 2 and 4 Gbit/s receivers were -36.6 and -31.2 dBm, respectively. These receivers used SAGM-APD with a gain-bandwidth product of 18 GHz, on ionization ratio k = 0.35, a dark current I_{dm} = 52 nA and a quantum efficiency η = 71%. The preamplifier employed high impedance GaAs FET.

The 8 Gbit/s receiver with -25.8 dBm sensitivity employed a SAGM-APD with a gain bandwidth product of 60 GHz, and a high impedance GaAs preamplifier. The SAGM-APD parameters were: ionization ratio k = 0.35, dark current I_{dm} = 52 nA and quantum efficiency η = 62%.

ACKNOWLEDGMENT

This work was performed as part of the program of the Electronics Research and Development Group, Electronics Engineering Department of the Lawrence Berkeley Laboratory, University of California, Berkeley. The work was partially supported by the U.S. Department of Energy under Contract Number DE-AC03-76SF00098. Reference to a company or product name does not imply approval or recommendation of the product by the University of California or the U.S. Department of Energy to the exclusion of others that may be suitable.

REFERENCES

1. A.H. Gnauck, J.E. Bowers, and J.C. Campbell, 8-Gbit/s Transmission over 30 km of Optical Fiber, Electron Lett., 22, pp. 600-602 (1986).

2. A.H. Gnauck, B.L. Kasper, R.A. Linke, R.W. Dawson, T.L. Koch, T.J. Bridges, E.G. Buckhard, R.T. Yen, D.P. Wilt, J.C. Campbell, K. Ciemecki Nelson and L.G. Cohen, 4-Gbit/s Transmission over 103 km of Optical Fiber Using a Novel Electronic Multiplexer/Demultiplexer, J. Lightwave Technology, LT-3, pp. 1032-1035, (October 1985).

3. B. Leskovar, M. Nakamura and B.T. Turko, Optical Wide Band Data Transmission System, Lawrence Berkeley Laboratory Report, LBL-23113, (March 15, 1987).

4. B. Leskovar, M. Nakamura and B.T. Turko, Wide Band Data Transmission System Using Optical Fibers, IEEE Trans. Nucl. Sci., NS-35, No. 1, pp. 334-341 (1988).

5. M. Nakamura, B. Leskovar and B.T. Turko, Signal Processing for an Optical Wide Band Data Transmission System, IEEE Trans. Nucl. Sci., NS-35, No. 1, pp. 197-204 (1988).

6. B. Leskovar, Radiation Effects on Optical Data Transmission System, Lawrence Berkeley Laboratory Report, LBL-25062 (April 15, 1988).

7. B. Leskovar, M. Nakamura, F.A. Kirsten and A.R. Clark, Study of Fiber Optics for Application to SSC Detector Systems, Lawrence Berkeley Laboratory Report, LBL PUB-5216 (August 18, 1988).

8. R.G. Smith and S.D. Personick, Receiver Design for Optical Fiber Communication Systems, Semiconductor Devices for Optical Communication, 39, pp. 89-160, Springer-Verlag (1987).

9. S.R. Forrest, Sensitivity of Avalanche Photodetector Receivers for High- Bit-Rate Long Wavelength Optical Communication Systems, in Semiconductors and Semimetals, 22, Academic Press, Part D, W.T. Tsang, Ed., pp. 329-381, (1985).

10. T.V. Muoi, Receiver Design For High Speed Optical-Fiber-Systems, J. Lightwave Technol., LT-2, pp. 243-267 (1984).

11. B.L. Kasper, and J.C. Campbell, Multigigabit-per-Second Avalanche Photodiode Lightwave Receivers, J. Lightwave Technol., LT-5, No. 10, pp. 1351-1364 (1987).

12. M. Kobayashi, H. Machida, T. Shirai, Y. Kishi, N. Takagi, and T. Kaneda, Optimized GaInAs Avalanche Photodiode With Low Noise and Large Gain-bandwidth Product, Proc. 6th Int. Conf. Integrated Opt. and Opt. Fiber Commun, paper MJ3, (Reno, NV), (1987).

13. J.C. Campbell, W.S. Holden, G.J. Qua, and A.G. Dentai, Frequency Response of InP/InGaAsP/InGaAs Avalanche Photodiodes with Separate Absorption Grading, and Multiplication Regions, IEEE J. Quantum Electron, QE-21, pp. 1743-1746 (1985).

14. T. Kaneda, Silicon and Germanium Avalanche Photodiodes, Semiconductor and Semimetals, 22, Part D, W.T. Tsang, Ed., pp. 247-328, Academic Press (1985).

15. J.C. Campbell, W.T. Tsang, G.J. Qua and J.E. Bowers, In/InGaAsP/InGaAs Avalanche Photodiode with 70 GHz Gain-Bandwidth Product, App. Phys. Lett., 51, (18), pp. 1454-1456 (2 Nov. 1987).

16. J. Yamada, A. Kawana, T. Mija, J. Nagai, and T. Kimura, Gigabit/s Optical Receiver Sensitivity and Zero Dispersion Single-Mode Fiber Transmission at 1.55 μm, IEEE J. Quantum Electronics. QE-18, pp. 1537-1546 (1982).

17. M. Shikada, S. Fujita, I. Takano, N. Heumi, I. Mito, K. Taguchi and K. Minemura, 1.5 μm High-Bit-Rate Long Span Transmission Experiments Employing a High-Power DFB-DC-PBH Laser Diode, Proc. 5th Int. Conf. Integrated Opt. and Opt. Fiber Commun., Venice, Italy (1985).

18. I.Takano, I. Mito, K. Taguchi, T. Watanabe and B. Hirosaki, A 4-Gbit/s Optical Regenerative Repeater for its Fiber Transmission Experiment, Proc. 6th Int. Conf. Integrated Opt. and Opt. Fiber Commun., 3, pp. 296-299 (1987).

19. S. Fujita, I. Takano, N. Heumi, Shikada, I. Mito, K. Taguchi and K. Minemura, 4 Gbit/s Long Span Transmission Experiments Employing High Speed DFB-LD's and InGaAs-APD's, Proc. 12th Enr. Conf. Optical Commun., Barcelona, Spain (1986).

20. B.L. Kasper, J.C. Campbell, J.R. Talman, A.H. Gnauck, J.E. Bowers and W.S. Holden, An APD/FET Optical Receiver Operating at 8 Gbit/s, J. Lightwave Technology., LT-5, pp. 344-347 (1987).

Table 1. Typical Characteristics of Photodetectors for Optical Receiver

	Si APD[a]	InGaAs APD[b]	InGaAs PIN[b]	SAGM-APD[b]
Quantum efficiency (%)	80	80	80	75-95
Capacitance (pF)	1	0.5	0.5	0.1-0.2
Dark current I_{ds} (nA)	1	1-5	1-5	
Dark current I_{dm} (nA)	0.001	1-5		2-50
Ionization ratio	0.02-0.03	0.3-0.5		0.35

[a] 800-900 nm wavelength range, [b] 1000-1500 nm wavelength range.

Table 2. State-of-the Art Optical Receiver Sensitivities

Bit Rate (Mbit/s)	Wavelength (nm)	Sensitivity[a] (dBm)	Detector	Amplifier[b]	Reference
400	1300	-40.2[c]	Ge APD	Si Bipolar-LZ	(16)
420	1510	-46.2[d]	InGaAs APD	GaAs FET-HZ	(11)
565	1540	-42.9[c]	InGaAs APD	GaAs FET-TZ	(17)
1000	1510	-42.1[d]	GaAs APD	GaAs FET-HZ	(11)
1200	1540	-40.0[c]	InGaAs APD	GaAs FET-HZ	(17)
2000	1510	-36.6[d]	InGaAs APD[e]	GaAs FET-HZ	(11)
2000	1540	-37.4[c]	InGaAs APD	GaAs FET-HZ	(17)
4000	1300	-29.1[c]	InGaAs APD	GaAs FET-TZ	(18)
4000	1510	-31.2[d]	InGaAs APD[e]	GaAs FET-HZ	(11)
8000	1300	-15.5[d]	InGaAs APD	GaAs FET-LZ	(1)
8000	1300	-25.8[d]	InGaAs APD[e]	GaAs FET-HZ	(20)

[a] For 10^{-9} bit error rate.

[b] HZ-high impedance, TZ-transimpedance, LZ-low impedance.

[c] Return-to-zero (RZ) digital coding format.

[d] Non-return-to-zero (NRZ) coding format.

[e] SAGM-APD.

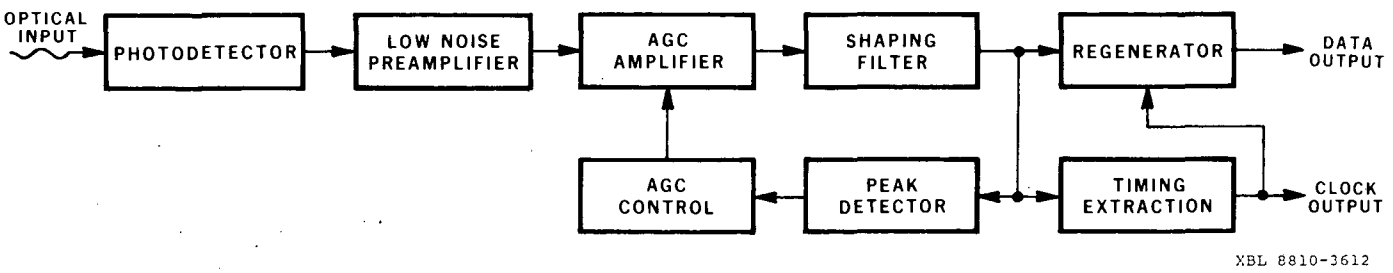

Fig. 1. Simplified block diagram of a typical digital optical receiver.

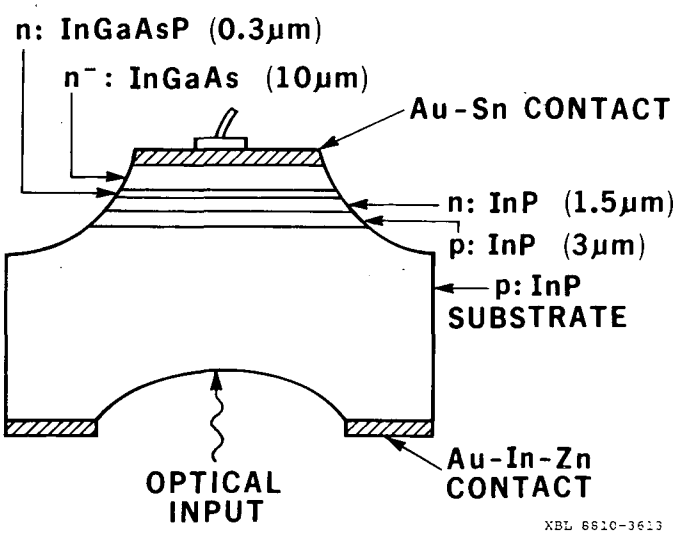

Fig. 2. Schematic Cross Section of an InP/InGaAsP/InGaAs SAGM-APD.

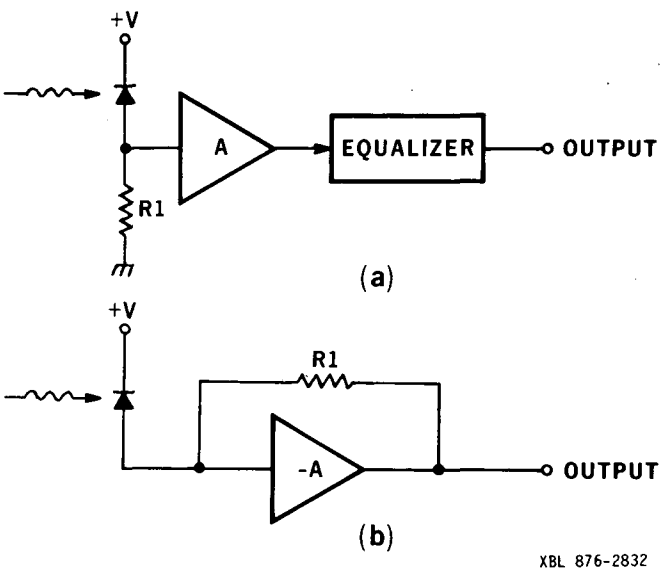

Fig. 3. (a) High impedance and (b) transimpedance designs of optical receiver preamplifier.

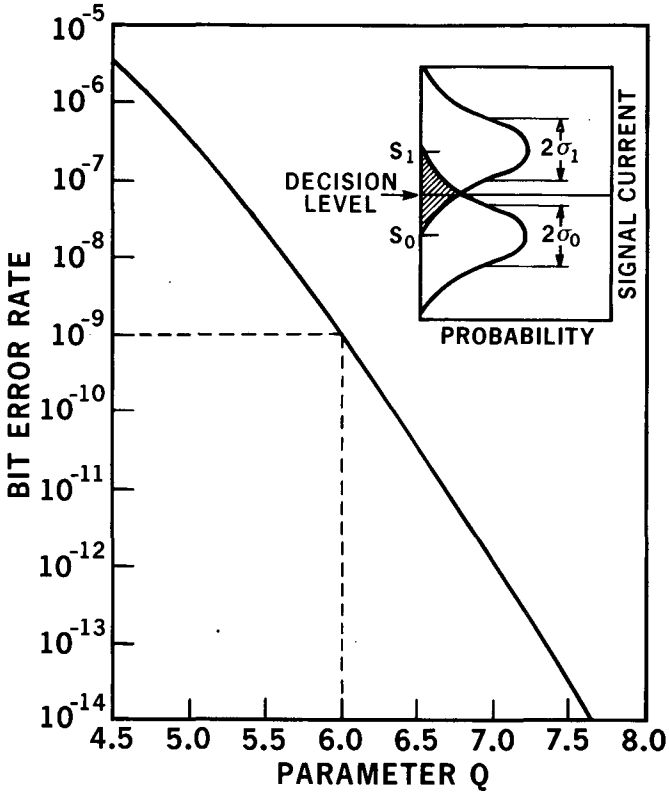

Fig. 4. Bir-error rate as a function of a parameter Q. Inset: Signal current S corresponding to a mark and a space indicating the variance σ and decision level D. The shaded area in the tails of distribution overlapping decision level indicated the probability for detecting an error.

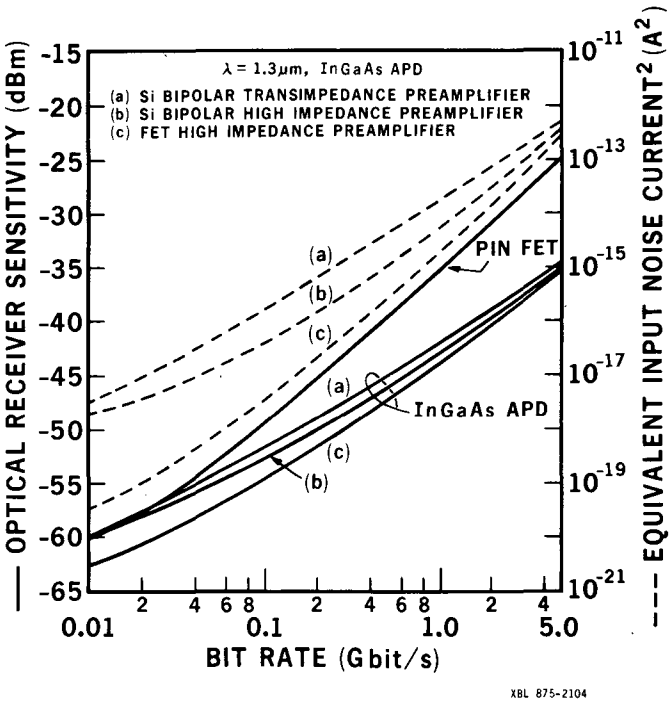

Fig. 5. Optical receiver sensitivity and equivalent input noise power versus operating bit rate.

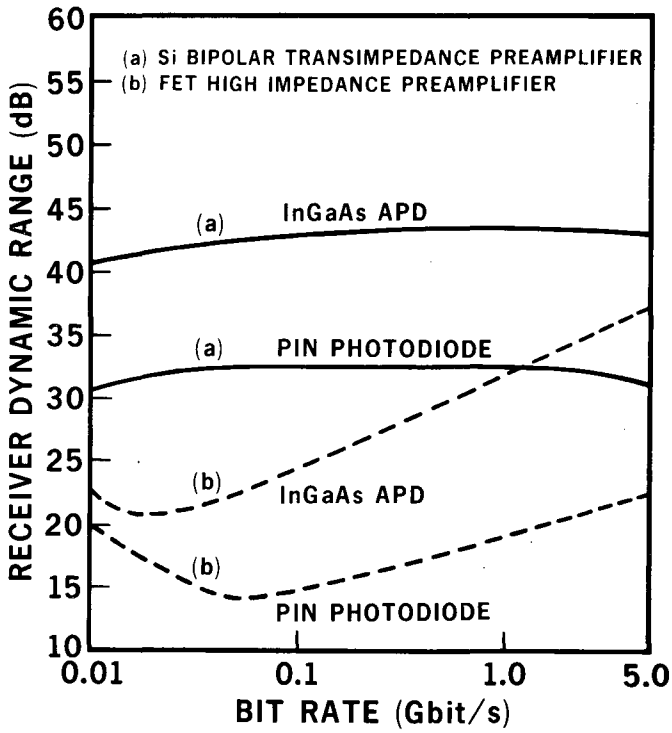

Fig. 6. Dynamic range of optical receiver as a function of the operating bit rate.

LAWRENCE BERKELEY LABORATORY
TECHNICAL INFORMATION DEPARTMENT
UNIVERSITY OF CALIFORNIA
BERKELEY, CALIFORNIA 94720